

The Plastic Origin of van der Waals material GaGeTe

Qiao Wang^{1,2}, *Ping-An Hu*^{1,3*}

1. Key Laboratory of Micro-systems and Micro-structures, Manufacturing of Ministry of Education, Harbin Institute of Technology, Harbin 150001, China
2. School of Chemistry and Chemical Engineering, Harbin Institute of Technology, Harbin 150001, China
3. School of Materials Science and Engineering, Harbin Institute of Technology, Harbin 150001, China

KEYWORDS: plastic inorganic semiconductors, van der Waals materials, layered materials, ductile materials, plastic mechanisms, flexible, germanium-based

ABSTRACT

This work reports the discovery of high plasticity in ternary germanium-based single-crystal GaGeTe, which breaks through the inherent brittleness of traditional binary germanium-based chalcogenides and fills a research gap in germanium-based plastic semiconductors. Combining spherical aberration-corrected transmission electron microscopy experiments with density functional theory calculations, the study reveals a novel deformation mechanism co-dominated by intralayer lattice distortion and interlayer slip. These findings provide fresh insight into the plastic behavior of inorganic semiconductors and clarifies the critical role of intralayer structural evolution in plastic behavior. This work not only expands the family of plastic semiconductor materials but also provides a new theoretical basis and candidate platform for the material design of flexible electronic devices.

1. Introduction

The emergence of plastic inorganic semiconductors has opened new possibilities for flexible electronics. Conventional inorganic semiconductors exhibit excellent electrical properties but suffer from intrinsic brittleness, while organic semiconductors offer mechanical flexibility but often lack sufficient carrier mobility and stability. Plastic inorganic semiconductors bridge this gap, showing great potential in flexible and wearable devices, like thermoelectric devices¹, touchscreens², X-ray detectors³, and ferromagnetic semiconductors⁴. However, reported plastic inorganic semiconductors are mostly limited to binary systems⁵ (e.g., Ag₂S⁶, ZnS⁷, InSe⁸, GaTe⁹, AgCl/Br¹⁰, Mg₃Bi₂¹¹) and their doped variants¹², whereas single-crystalline materials with ternary

or higher compositions remain rare. Multicomponent single crystals offer a broader chemical design space, opening a new dimension for the precise customization of plastic semiconductors. Particularly taking germanium (Ge)-based materials as an example, Ge-based semiconductors are crucial for electronics and optoelectronics,¹³ yet their binary sulfides, selenides and tellurides are typically brittle,⁵ and no Ge-based plastic semiconductor has been reported to date. However, we discovered ultra-high plasticity in ternary Ge-containing single crystal GaGeTe.

Moreover, current studies on deformation mechanisms in plastic inorganic semiconductors predominantly focus on classical theories, such as dislocation glide⁸, phase transitions¹⁴, twinning⁷, and amorphization^{9,15}, with an emphasis on interlayer slip and grain boundary behavior, while the role of intralayer lattice distortion remains underexplored. In this work, we study GaGeTe as a model plastic semiconductor. Using spherical aberration corrected transmission electron microscope (AC-TEM) experiments and density functional theory (DFT) theoretical studies, we uncover a unique deformation mechanism in plastic inorganic semiconductors: plasticity is co-dominated by intralayer lattice distortion and interlayer slip. This finding not only expands the family of plastic semiconductors but also provides new insights into their deformation mechanisms.

2. Results and Discussion

GaGeTe is an emerging ternary layered semiconductor that has recently demonstrated broad application prospects in fields such as thermoelectric conversion, infrared optoelectronics, and topological quantum materials.¹⁶ This material possesses a typical hexagonal layered structure (Figure 1a), belonging to the R-3m space group with lattice parameters of $a = 4.05 \text{ \AA}$ and $c = 34.65 \text{ \AA}$. Within each individual layer, Ge atoms form a germanene-like hexagonal layer, which is sandwiched between GaTe layers, resulting in a Te–Ga–Ge–Ge–Ga–Te stacking sequence. These

structural layers are coupled along the c-axis via weak van der Waals interactions. GaGeTe can be prepared either by chemical vapor transport (CVT) or directly grown via the Bridgman method. However, both approaches often struggle to yield pure GaGeTe. Due to its layered structure like that of GaTe and the comparable van der Waals forces involved, trace amounts of GaTe crystals are frequently incorporated during crystallization. To avoid interference from GaTe, we can only select mechanically separated GaGeTe samples that show no peak at $2\theta = 24^\circ$ (the characteristic peak of GaTe) in the XRD pattern (Figure S1) for mechanical testing.

The three-point bending test results of GaGeTe (Figure 1b) reveal its unique mechanical behavior. The material exhibits significant plastic deformation capacity, achieving an engineering strain of 7.5% without fracture (Figure 1a), yet its yield strength is extremely low, only approximately 6 MPa. This strength value is several tens of times lower than that of polycrystalline copper, highlighting its intrinsically soft nature. The ability to undergo large deformation without fracture is primarily attributed to its layered structure. The acute angles formed on both sides of the deformed specimen visually demonstrate extensive interlayer slip between van der Waals-bonded layers during the bending process, which effectively dissipates stress. This finding is highly consistent with previous literature on the deformation mechanisms of layered materials.⁵ Furthermore, GaGeTe demonstrates remarkable fracture resistance even under extreme stress. As shown in Figure c, bulk GaGeTe crystals can be wrapped around a needle with a radius of only 0.35 mm without fracture, fully demonstrating their macroscopic plasticity. This characteristic makes GaGeTe unique among germanium-based semiconductors: according to the plasticity-brittleness statistics presented in Figure d, GaGeTe is, to our knowledge, the only germanium-based semiconductor discovered to date that exhibits such plasticity.

To gain deeper insights into the structural origins of the unique macroscopic plasticity in GaGeTe, we conducted a series of multi-scale characterizations. Figure 2a shows scanning electron microscopy (SEM) images that visually confirm its exceptional flexibility: an initially flat layered crystal can be bent into a "Z"-shape without fracture, retaining only creases upon unbending. The sharp-angled morphology at the bent edges, clearly visible and resulting from interlayer slip, correlates with the observations from the macroscopic three-point bending test (Figure 1b), collectively identifying van der Waals interlayer slip as the primary deformation mechanism. To capture this slip process at a finer scale, we performed eccentric micro compression tests on pillars oriented along the c-axis. Figure 2b reveals that the sidewalls of the compressed GaGeTe micropillars (approximately 1.5 μm in diameter) exhibit a distinct step-like morphology, providing direct microscopic evidence of relative slip between the layers. A corresponding schematic diagram of the slip model is presented in Figure 2c.

Theoretical calculations unveiled the fundamental reason for its facile slip from an energy perspective. Density functional theory (DFT) calculations yielded the interlayer slip energy for GaGeTe, which is as low as approximately 0.026 eV/atom, as shown in Figure 2d. This ultralow slip energy is key to its macroscopic softness. As demonstrated in the comparison with various materials in Figure 2e, the slip energy of GaGeTe is comparable to that of known plastic van der Waals materials (e.g., SnSe₂, \sim 0.022 eV/atom) and is significantly lower than that of typical plastic inorganic semiconductors like Ag₂S (\sim 0.166 eV/atom). For comparison, we calculated the slip energy for chemically similar GeTe, which is much higher, at \sim 0.234 eV/atom. However, the brittleness of GeTe is not solely attributable to its high slip energy. Compression experiments revealed that GeTe readily forms a corrugated, "corrugated paper"-like structure in its cross-section upon deformation (Figure S2). The formation of this structure further physically hinders

slip propagation, collectively leading to its brittle behavior. In summary, the extremely low interlayer slip energy combined with a stable layered structure confers upon GaGeTe this unprecedented plastic deformability among germanium-based semiconductors.

We further investigated the stability and evolution mechanism of the GaGeTe monolayer structure at the atomic scale under deformation using high-angle annular dark-field scanning transmission electron microscopy (HAADF-STEM). As shown in Figure 3a, a cross-sectional transmission electron microscopy (TEM) lamella was prepared from a fold of the GaGeTe single crystal via focused ion beam (FIB) milling. The bright-field (BF) TEM image of the fold cross-section (Figure 3b) reveals that stress concentration during interlayer slip led to the formation of local bulges, accompanied by underlying interlayer cleavage. The BF image shows that some regions experienced slip without significant deformation, while other regions developed pronounced kinking-like bulge structures.

To compare the atomic structure before and after deformation, HAADF-STEM imaging was performed on both the undeformed matrix (Figure 3c) and the kinked region (Figure 3e). Since the intensity of individual atomic columns is approximately proportional to $Z^{1.7}$ (where Z is the atomic number), the contrast from Ga ($Z=31$) and Ge ($Z=32$) is significantly weaker than that from Te ($Z=52$), making them nearly invisible along the $[-110]$ zone axis. Both regions maintain a clear single-crystal structure with orderly atomic arrangement; however, the atomic configuration in the kinked region exhibits a unique "racetrack"-like pattern. Notably, the lattice remains devoid of dislocations or other line defects. Selected area electron diffraction (SAED) analysis (Figure 3d) further confirms that even with a bending angle of up to 31° , no defects such as twinning, phase transitions, or amorphization were observed, demonstrating the excellent ability of the GaGeTe monolayer to preserve its crystalline integrity at the atomic scale.

The fundamental reason for this phenomenon lies in the GaGeTe monolayer's ability to tolerate substantial intralayer lattice distortion. As shown in Figure 3f, comparing the interplanar spacings from the stress-concentrated center of the kink with those from the undeformed region reveals that bending compresses the intralayer thickness of GaGeTe by tens to hundreds of picometers, while the interlayer spacing increases by on the order of 80-90 picometers. Analysis of a magnified view of the kink center (Figure 3g) indicates that the bending strain distributes unevenly within a single layer: the upper part experiences compressive stress, shortening the atomic bond lengths, while the lower part experiences tensile stress, elongating the bonds. This strain exhibits a regular distribution across the layers: the increased bond lengths in the tensile-strained lower part of each layer result in its overall length being greater than that of the compressive-strained upper part of the subjacent layer. This asymmetric strain accumulates progressively in the vertical direction, ultimately leading to the formation of sharp angles at the macro-scale.

To visualize this deformation mechanism more intuitively, we constructed a simplified ball-and-spring model (Figures 3h, 3i). In this model, the chemical bonds in GaGeTe are abstracted as elastic springs that undergo bond length stretching/compression and bond angle changes under bending strain. The model clearly demonstrates that continuous and coordinated intralayer lattice distortion is the key reason enabling GaGeTe to achieve large-angle bending without fracture while maintaining its crystal structure, thereby elucidating the origin of its exceptional plastic deformability at the atomic scale.

Based on the systematic investigation of the macroscopic plasticity, microscopic slip, and atomic-scale lattice distortion of GaGeTe presented in the preceding sections, we finally employed the Crystal Orbital Hamiltonian Population (COHP) method within Density Functional Theory

(DFT) calculations to deeply explore the origin of the dramatic difference in mechanical performance—brittleness versus ductility—between two van der Waals materials with similar elemental compositions: GeTe and GaGeTe.

To facilitate computation and quantitatively assess the stability of chemical bonds under tensile strain, we transformed the crystal structures of GeTe and GaGeTe into orthogonal models. We systematically computed the Crystal Orbital Hamiltonian Population (COHP) and its integrated form (-ICOHP) for the following: the Ge–Te bond in undeformed GeTe; the Ga–Te, Ga–Ge, and Ge–Ge bonds in undeformed GaGeTe; and, as a reference, the Ge–Ge bond in germanene. Corresponding calculations were also performed for the Ge–Te bond in GeTe and the Ga–Te, Ga–Ge, and Ge–Ge bonds in GaGeTe under 5% and 10% tensile strain along the a-axis and b-axis in the orthogonal structure. The absolute value of -ICOHP is a key metric for assessing chemical bond strength, where a larger value indicates stronger bonding interaction.

Comparison of their crystal structures (Figure 4a) reveals that GeTe is composed solely of Ge–Te bonds, whereas the bonding pattern in GaGeTe is more diverse, consisting of Ga–Te, Ga–Ge, and Ge–Ge bonds. As shown in Figure 4b, within the 10% tensile strain range, the -ICOHP values for all chemical bonds decrease with increasing strain, indicating a weakening of the bonding interactions. However, the crucial distinction lies in the fact that even when stretched to 10%, the -ICOHP values for the Ga–Te, Ga–Ge, and Ge–Ge bonds in GaGeTe all remain above 3 eV, substantially higher than the -ICOHP value of the undeformed Ge–Te bond (only 1.32 eV). This demonstrates that the Ge–Te bond is inherently weak and prone to fracture under stress, directly leading to the macroscopic brittleness of GeTe.

In contrast, although GaGeTe contains Ge elements, its successful bonding design completely avoids the fragile Ge–Te bond. Instead, the Ge atoms form strong and ductile Ge–Ge and Ga–Ge bonds with metallic character with themselves and Ga atoms, fundamentally ensuring the material's deformability at the chemical bond level. This conclusion is further corroborated by the COHP curves (Figure 4c): compared to the tall bonding peaks below the Fermi level for the Ga–Te and Ga–Ge bonds in GaGeTe, and the Ge–Ge bonds in both GaGeTe and germanene, the bonding peak for the Ge–Te bond is significantly lower and weaker. It is particularly noteworthy that the intensity of the bonding peak for the Ge–Ge bond in GaGeTe closely resembles that of the Ge–Ge bond in germanene, which is renowned for its flexibility. This strongly suggests that such strong covalent bonds provide crucial structural support for the macroscopic plasticity of GaGeTe.

3. Conclusions

In summary, this study, proceeding from a multi-scale analysis and culminating at the fundamental level of chemical bonding, reveals the origin of GaGeTe's exceptional plasticity: its unique "sandwich" layered structure avoids the formation of brittle Ge–Te bonds, instead constructing a stable bonding network comprised of strong and resilient Ga–Te, Ga–Ge, and metal-like Ge–Ge bonds. This discovery not only explains the divergent mechanical properties of GaGeTe and GeTe but also provides key guidance for bonding engineering in the future design of novel plastic semiconductor materials.

4. Experimental Methods

Growth of single-crystal GaGeTe:

High-purity Ga (5N, 99.999%), Ge (5N, 99.999%), and Te (5N, 99.999%) were obtained from ZhongNuo Advanced Material (Beijing) Technology Co., Ltd., and used as raw materials. Stoichiometric amounts of Ga, Ge, and Te (with a molar ratio of Ga : Ge : Te = 1 : 1 : 1) were loaded into a carbon-coated quartz ampoule under vacuum, which was then flame-sealed. The internal pressure of the ampoule after vacuum encapsulation was 1000 Pa. The synthesis was carried out in a programmable tube furnace using the following thermal protocol: the temperature was first raised to 950 °C at a rate of 10 °C/min and held for 12 hours for homogenization; then slowly increased to 980 °C at 1 °C/min and maintained at this temperature for 3 days to ensure complete reaction. Subsequently, the sample was cooled to 850 °C at 5 °C/min, followed by a slow cooling step over 7 days down to 750 °C, and finally cooled to room temperature.

Characterization: The initial sample dimensions for three points bending engineering stress-strain tests are using Instron ® 5566 universal testing machine with a constant loading rate of 0.05 mm min⁻¹. The scanning electron microscope (SEM) images were carried out on ZEISS Merlin Compact. The transmission electron microscopy (TEM) and spherical aberration corrected transmission electron microscopy (AC-TEM) data of BiSeI were obtained using the Talos F200X and JEM-ARM200F NEOARM. The TEM samples were done by a focused ion beam (FIB, FEI Helios NanoLab 600i DualBeam). Optical photographs were taken by VIVO IQOO Z7I. The GaTe crystal was examined by X-ray diffraction using Cu Ka Source (Panalytical Instruments, X'PERT).

DFT computational details: The density functional theory (DFT) is implemented by the Vienna ab initio simulation package (VASP). The electronic exchange-correlation effects were described with the generalized gradient approximation of the Perdew-Burke-Ernzerhof (PBE) functional with the generalized gradient approximation (GGA). The plane-wave cutoff energy was set to be 500 eV in all calculations, while the k-points mesh based on the Gamma-centered method was set

to be $3 \times 12 \times 5$. The convergence criteria for energy and force were set as 1×10^{-6} eV 0.02 eV/Å.

Notes

The authors declare no competing financial interest.

REFERENCES

- (1) Qiu, P.; Deng, T.; Chen, L.; Shi, X. Perspective Plastic Inorganic Thermoelectric Materials. *Joule* **2024**, *8* (3), 622–634. <https://doi.org/10.1016/j.joule.2023.12.020>.
- (2) Zhao, X.; Yang, S.; Wen, X.; Huang, Q.; Qiu, P.; Wei, T.; Zhang, H.; Wang, J.; Zhang, D. W.; Shi, X.; Lu, H. A Fully Flexible Intelligent Thermal Touch Panel Based on Intrinsically Plastic Ag₂S Semiconductor. **2022**, *2107479*, 1–7. <https://doi.org/10.1002/adma.202107479>.
- (3) Wang, Q.; Wan, C.; Wu, Y.; Fan, X.; Wang, S.; Pan, Y.; Khalid, M.; Xiao, H.; Zhang, H.; Ma, G.; Fu, Y.; Hu, P. Plastic Inorganic van Der Waals Semiconductors for Flexible X - Ray Detectors. **2025**. <https://doi.org/10.1021/acsaelm.4c01931>.
- (4) Luo, J.; Chen, J.; Gao, Z.; Zhou, J.; Zhang, J.; Qiu, P.; Shen, S.; Dong, S.; Chen, L.; Shi, X. Ductile Inorganic Ferromagnetic Semiconductor. *Advanced Materials* **2025**, *14083*, 1–9. <https://doi.org/10.1002/adma.202514083>.

- (5) Gao, Z.; Wei, T. R.; Deng, T.; Qiu, P.; Xu, W.; Wang, Y.; Chen, L.; Shi, X. High-Throughput Screening of 2D van Der Waals Crystals with Plastic Deformability. *Nature Communications* **2022**, *13* (1). <https://doi.org/10.1038/s41467-022-35229-x>.
- (6) Shi, X.; Chen, H.; Hao, F.; Liu, R.; Wang, T.; Qiu, P.; Burkhardt, U.; Grin, Y.; Chen, L. Room-Temperature Ductile Inorganic Semiconductor. *Nature Materials* **2018**, *17* (5), 421–426. <https://doi.org/10.1038/s41563-018-0047-z>.
- (7) Oshima, Y.; Nakamura, A.; Matsunaga, K. Extraordinary Plasticity of an Inorganic Semiconductor in Darkness. **2018**, No. May, 2–4.
- (8) Wei, T. R.; Jin, M.; Wang, Y.; Chen, H.; Gao, Z.; Zhao, K.; Qiu, P.; Shan, Z.; Jiang, J.; Li, R.; Chen, L.; He, J.; Shi, X. Exceptional Plasticity in the Bulk Single-Crystalline van Der Waals Semiconductor InSe. *Science* **2020**, *369* (6503), 542–545. <https://doi.org/10.1126/science.aba9778>.
- (9) Tan, J.; Zhang, H.; Wang, X.; Wang, Y.; Wang, J. Deformable Monoclinic Gallium Telluride with High In-Plane Structural Anisotropy. **2024**, *80* (November). <https://doi.org/10.1016/j.mattod.2024.08.029>.
- (10) Huang, H.; Chen, H.; Gao, Z.; Ma, Y.; Zhao, K. Room-Temperature Wide-Gap Inorganic Materials with Excellent Plasticity. **2023**, *2306042*, 1–6. <https://doi.org/10.1002/adfm.202306042>.
- (11) Zhao, P.; Xue, W.; Zhang, Y.; Zhi, S.; Ma, X.; Qiu, J.; Zhang, T.; Ye, S.; Mu, H.; Cheng, J.; Wang, X.; Hou, S.; Zhao, L.; Xie, G.; Cao, F.; Liu, X.; Mao, J.; Fu, Y.; Wang, Y.;

- Zhang, Q. Plasticity in Single-Crystalline Mg₃Bi₂ Thermoelectric Material. *Nature* **2024**, *631* (8022), 777–782. <https://doi.org/10.1038/s41586-024-07621-8>.
- (12) Shen, K.; Yang, Q.; Qiu, P.; Zhou, Z.; Yang, S.; Wei, T. Ductile P-Type AgCu (Se , S , Te) Thermoelectric Materials. **2024**, *2*, 1–11. <https://doi.org/10.1002/adma.202407424>.
- (13) Kimerling, L. C.; T, G. *Related Titles Porous Silicon in Practice Preparation , Characterization and Silicon Photonics - The State of the Art*.
- (14) Sun, Y.; Ma, Y.; Rodney, D.; Xu, B. Van Der Waals Semiconductor InSe Plastifies by Martensitic Transformation. **2024**, *9593* (October), 1–8. <https://doi.org/10.1126/sciadv.ado9593>.
- (15) Wang, Y.; Li, A.; Hong, Y.; Deng, T.; Deng, P.; Huang, Y.; Liu, K.; Wang, J.; Fu, C.; Zhu, T. Iterative Sublattice Amorphization Facilitates Exceptional Processability in Inorganic Semiconductors. **2025**, *24* (October). <https://doi.org/10.1038/s41563-024-02112-7>.
- (16) Wang, W.; Li, L.; Zhang, Z.; Yang, J.; Tang, D.; Zhai, T. Ultrathin GaGeTe P-Type Transistors. **2017**, 1–4. <https://doi.org/10.1063/1.4998350>.

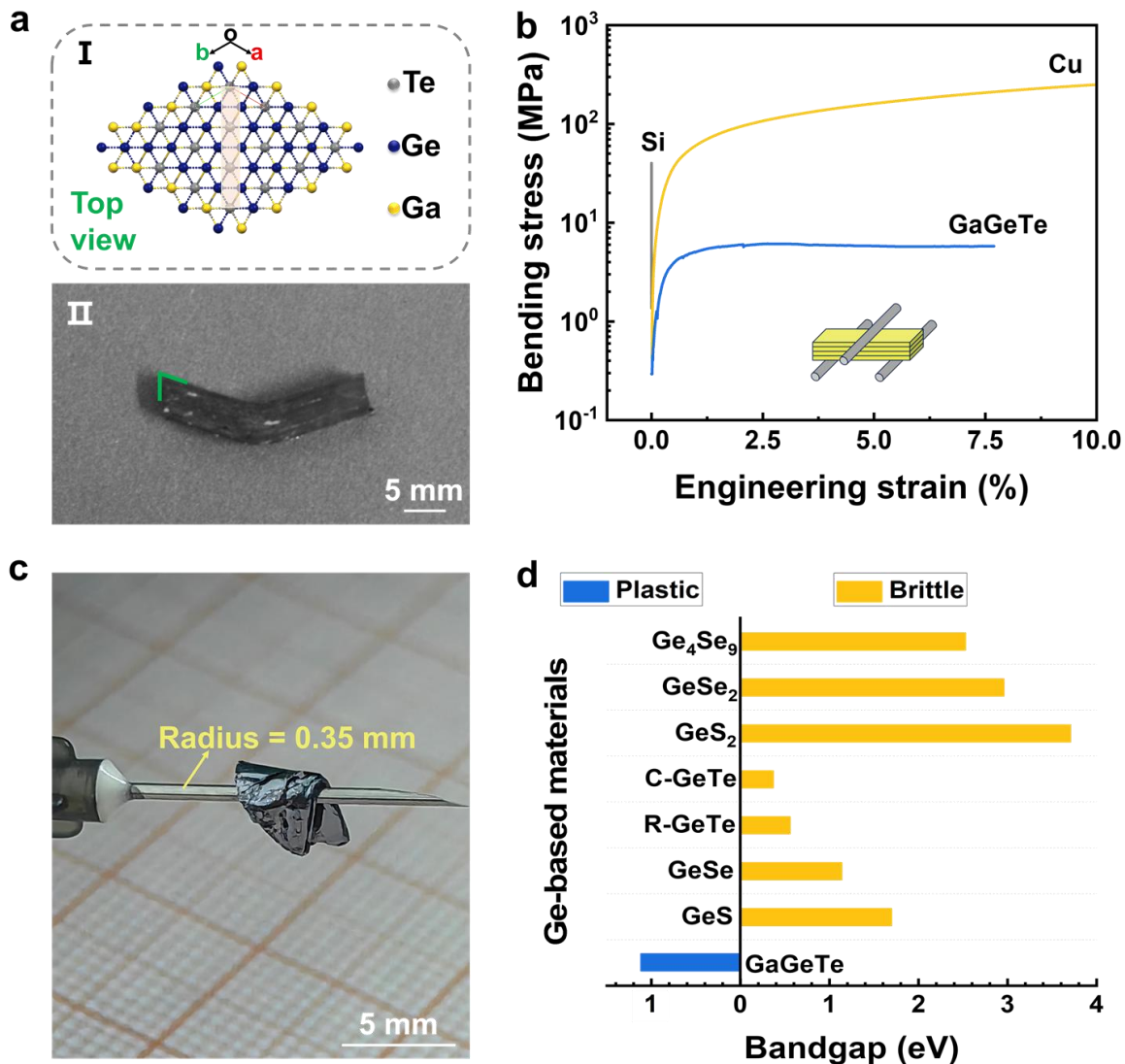


Figure 1. Deformability of GaGeTe single crystal. (a) Crystal structure and optical images of GaGeTe. (I) Crystal structure of GaGeTe with projection on the (001) plane. The pale pink shaded area indicates the crystal cutting direction for the three-point bending test. (II) Optical image of the corresponding bulk sample after the test, demonstrating plastic deformation without fracture. (b) Strain–stress curves for three-point bending test. Typical plastic material polycrystalline copper (Cu) is shown for comparison. The inset in (b) shows the applied force along the c axis of the crystals. (c) Optical image of a bulk GaGeTe single crystal being bent around a syringe needle (radius: 0.35 mm) without fracture. (d) Comparison of the deformability and bandgap of GaGeTe with other Ge-based materials. GaGeTe is the only Ge-based semiconductor material with good plastic deformation capability.

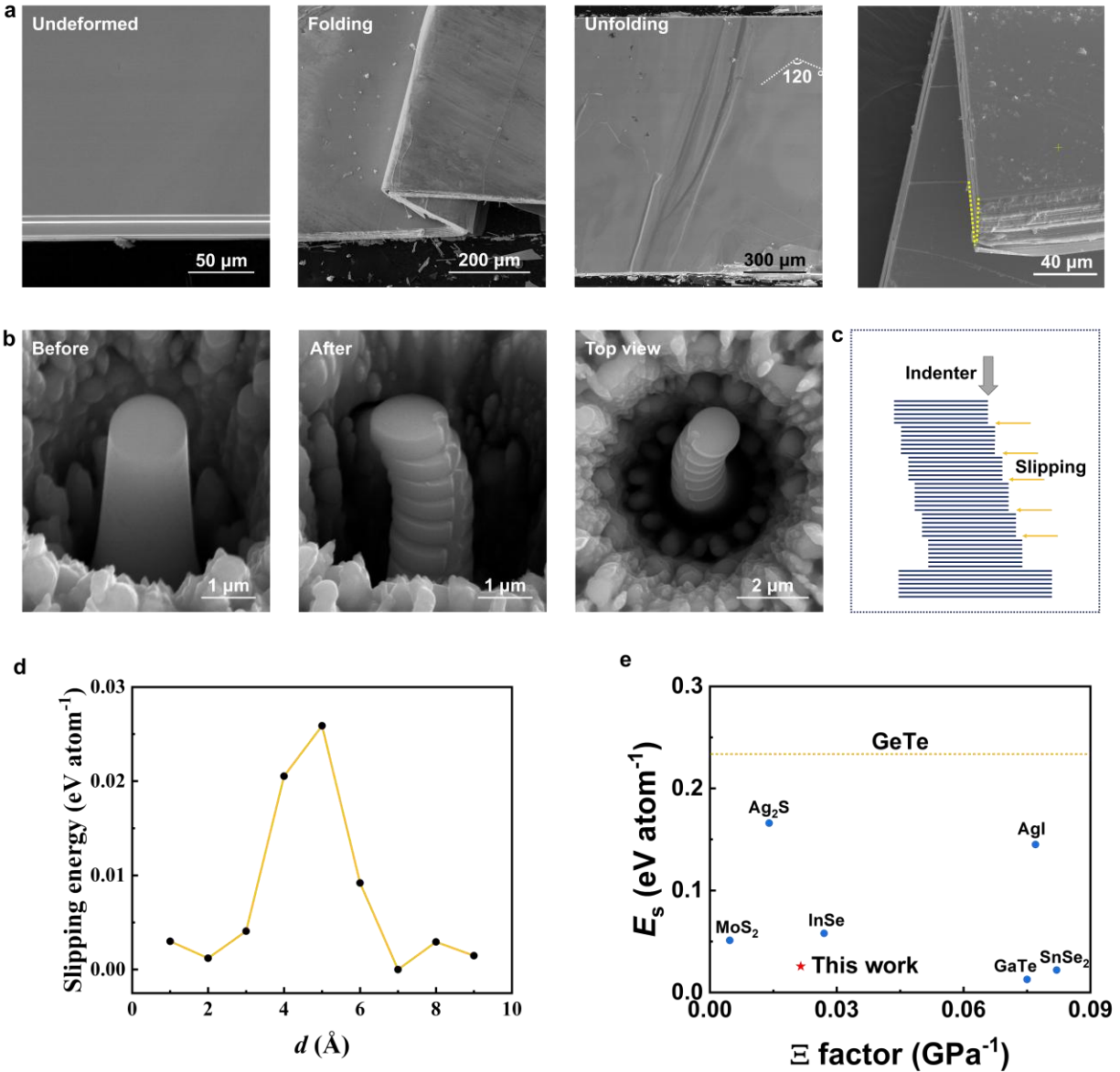


Figure 2. Interlayer slipping of GaGeTe micropillars under eccentric compression (a) SEM images of GaGeTe before and after deformation. (b) Eccentric compression test of a GaGeTe micropillar along the c-axis, revealing interlayer slipping. (c) Schematic diagram of the slipping mechanism induced by eccentric compression of a micropillar. (d) Slipping energy as a function of separating distance between a GaGeTe monolayer and a two-layer slab. (e) Comparison of the

deformability factor and slipping energy of GaGeTe with those of classical plastic van der Waals materials and similar elemental germanium-based brittle materials (GeTe, yellow dashed line).

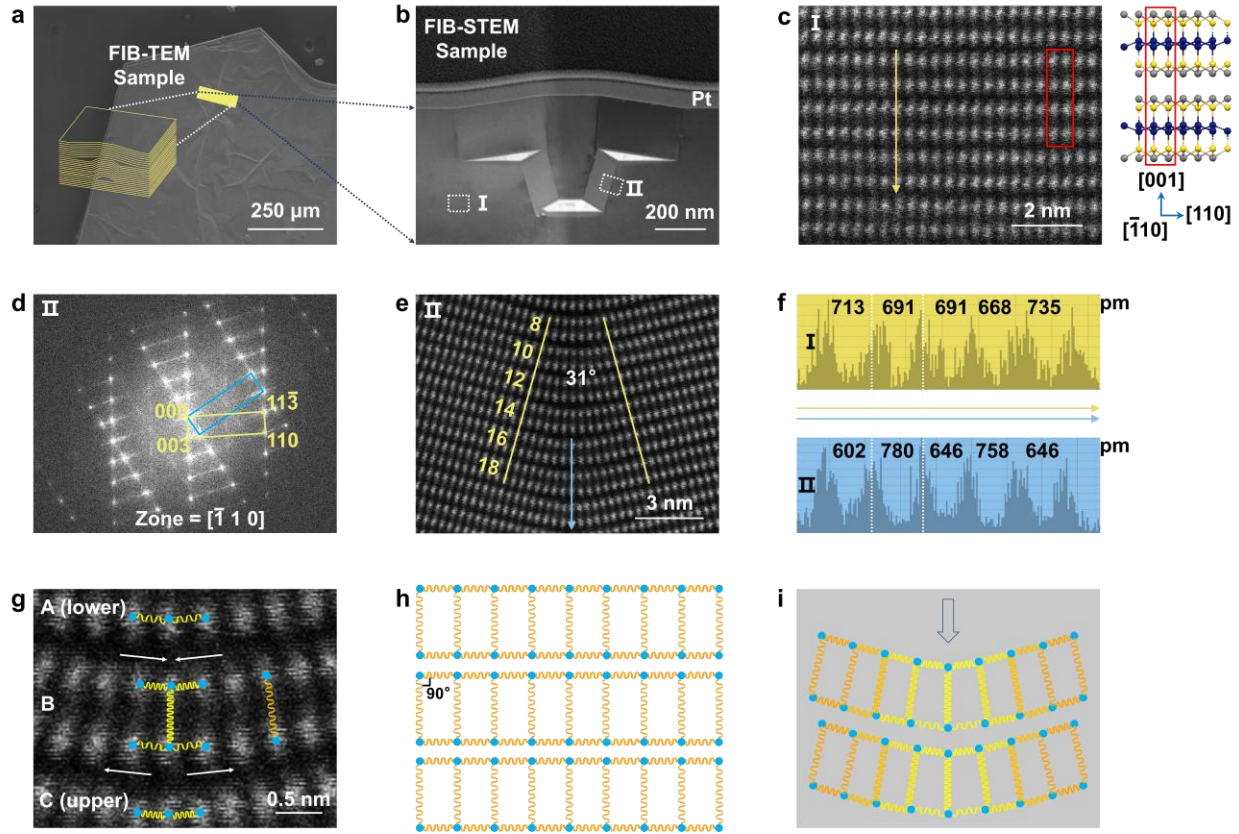


Figure 3. Atomic-scale characterization of the intralayer structural evolution in GaGeTe upon folding. (a) SEM image showing the location where the TEM lamella was prepared by FIB (at a fold in the GaGeTe sample). (b) Bright-field (BF) TEM image of the cross-sectional view of the folded GaGeTe lamella. (c) High-angle annular dark-field scanning transmission electron microscopy (HAADF-STEM) image corresponding to the undeformed matrix (labeled I) in panel (b). (d and e) Selected area electron diffraction (SAED) pattern and HAADF-STEM image taken from the folded region (labeled II) in panel (b), respectively. (f) Comparison of the measured interplanar spacings from the undeformed and folded regions. The arrows in (c) and (e) indicate the measurement locations. (g) Magnified view of the central area in the HAADF-STEM image of (e). (h and i) Schematic illustrations of the simplified spring models for the undeformed and folded GaGeTe lamella, respectively.

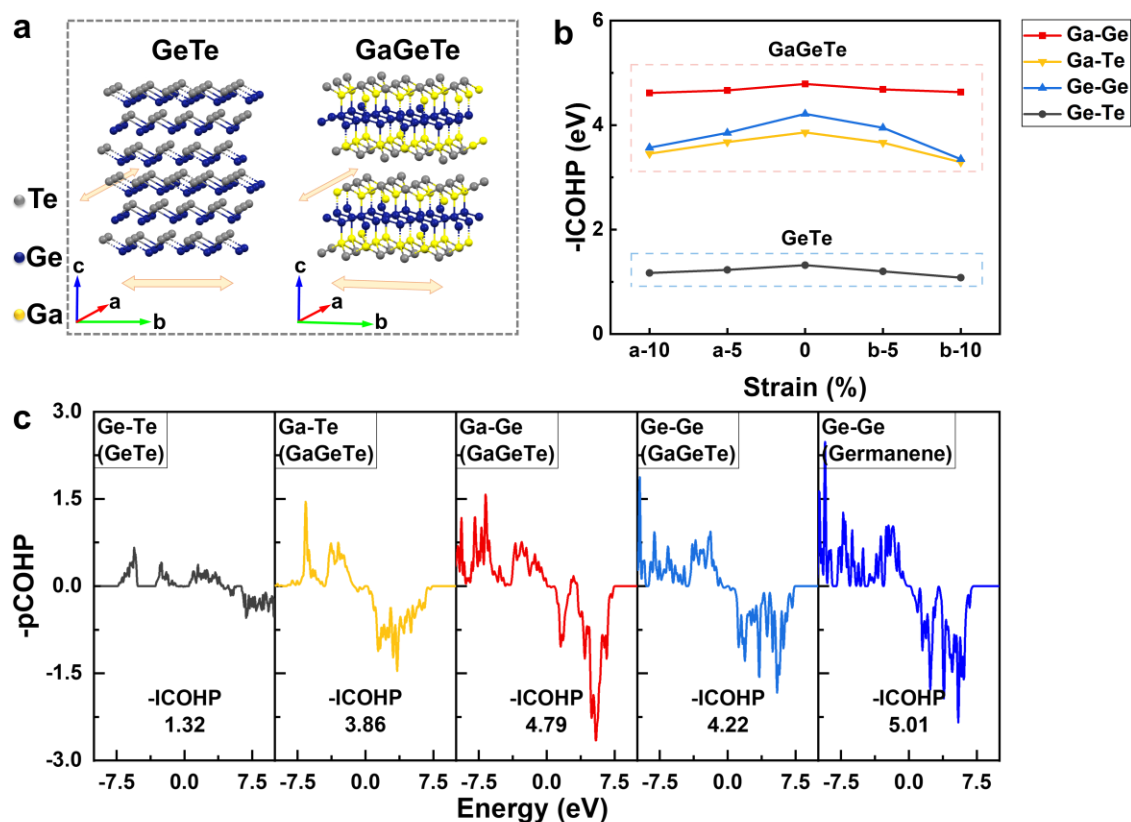


Figure 4. Inter-layer chemical bonding analysis. (a) Comparison of the crystal structures of GeTe and GaGeTe. (b) Variation of the -ICOHP values for different chemical bonds (the Ge–Te bond in GeTe; the Ga–Te, Ga–Ge, and Ge–Ge bonds in GaGeTe; and the Ge–Ge bond in germanene) as a function of tensile strain. (c) Crystal Orbital Hamiltonian Population (COHP) curves for the corresponding bonds.